



## Predictive Value of Quantitative Parameters in Evaluating Radiotherapy Efficacy for Hepatocellular Carcinoma Based on IQon Spectral CT: A Prospective Study

Jin Ying Lan<sup>1</sup> & Jin Han Yang<sup>1</sup>, Dong Wu Chen<sup>2</sup>, Jin Yuan Liao<sup>3</sup>

### Abstract

**Background:** Currently, there is a lack of reliable biomarkers for the early prediction of therapeutic response to radiotherapy in patients with hepatocellular carcinoma (HCC). Conventional imaging modalities are limited in their ability to detect early treatment-induced changes. IQon Spectral computed tomography (CT), as an advanced imaging technique, enables the acquisition of quantitative parameters, including iodine concentration and spectral curve slope, thereby providing a novel, non-invasive method for assessing tumor angiogenesis and metabolic activity. This study aims to prospectively evaluate the clinical utility of these quantitative parameters in predicting radiotherapy outcomes in HCC.

**Method:** This prospective study enrolled 30 patients with HCC who met the predefined inclusion and exclusion criteria were prospectively enrolled between July 2022 and June 2024. All patients received two cycles of radiotherapy and underwent IQon Spectral CT scans both before and after treatment. Based on the modified Response Evaluation Criteria in Solid Tumors (mRECIST), patients were classified into an effective group (complete response [CR] + partial response [PR]) and an ineffective group (stable disease [SD] + progressive disease [PD]). Changes in CT-derived quantitative parameters before and after radiotherapy were compared and analyzed, a predictive model for therapeutic efficacy was constructed, and receiver operating characteristic (ROC) curve analysis was performed to evaluate diagnostic performance.

**Results:** All 30 patients were diagnosed with HCC at clinical stages II–IV. Among them, 3 achieved CR, 19 achieved PR, 5 had SD, and 3 had PD. To evaluate the therapeutic efficacy of radiotherapy in HCC, three parameters—spectral curve slope (KAP), iodine content (ICAP), and normalized iodine concentration (NICAP)—were integrated during the arterial phase before treatment. Based on these parameters, five prediction models were constructed: bivariate models, a trivariate model, and a joint prediction model. The area under the curve (AUC) values were as follows: KAP\_ICAP model, 0.642 (95% CI: 0.410–0.874); KAP\_NICAP model, 0.886 (95% CI: 0.759–1); ICAP\_NICAP model, 0.898 (95% CI: 0.778–1); and KAP\_ICAP\_NICAP trivariate model, 0.915 (95% CI: 0.814–1), with a sensitivity of 86.4% and specificity of 87.5%. DeLong test results indicated that the predictive performance of the KAP\_ICAP\_NICAP model was significantly superior to that of the KAP\_ICAP model ( $Z = -2.396$ ,  $P = 0.017$ ), but no statistically significant differences were observed when compared with other bivariate models ( $P > 0.05$ ). The joint prediction model also achieved an AUC of 0.915 (95% CI: 0.810–1), with a sensitivity of 90.9%, specificity of 87.5%, positive predictive value

### Affiliation:

<sup>1</sup>Department of Radiology, Guiping People's Hospital, Guigang 537200, Guangxi Zhuang Autonomous Region, China

<sup>2</sup>Department of Ophthalmology, Guiping People's Hospital, No. 7 Renmin West Road, Guiping, Guigang 537200, Guangxi, China

<sup>3</sup>Department of Radiology, The First Affiliated Hospital of Guangxi Medical University, Nanning 530021, Guangxi Zhuang Autonomous Region, China

### Corresponding author:

Jin Ying Lan. Department of Radiology, Guiping People's Hospital, Guigang 537200, Guangxi Zhuang Autonomous Region, China.

# Jin Ying Lan and Jin Han Yang contributed equally to this work and should be considered co-first authors.

**Citation:** Jin Ying Lan, Jin Han Yang, Dong Wu Chen, Jin Yuan Liao. Predictive Value of Quantitative Parameters in Evaluating Radiotherapy Efficacy for Hepatocellular Carcinoma Based on IQon Spectral CT: A Prospective Study. *Journal of Radiology and Clinical Imaging*. 9 (2026): 1-9.

**Received:** January 19, 2026

**Accepted:** January 25, 2026

**Published:** February 04, 2026

of 95.2%, and negative predictive value of 77.8%. The DeLong test revealed no significant difference between the joint prediction model and the trivariate model ( $P = 0.999$ ), yet both outperformed the KAP\_ICAP model significantly ( $Z = -2.362$ ,  $P = 0.018$ ). In conclusion, models incorporating the NICAP parameter demonstrate high accuracy in predicting radiotherapy efficacy for HCC. Both the trivariate model and the ensemble learning-based joint prediction model exhibit excellent predictive performance and can serve as reliable quantitative tools for clinical assessment of treatment outcomes.

**Conclusion:** Quantitative parameters derived from IQon Spectral CT scan sensitively reflect early radiological changes associated with radiotherapy in HCC. The findings confirm that pretreatment IQon Spectral CT parameters, especially NICAP, can noninvasively and sensitively predict early treatment response to radiotherapy in HCC, offering a reliable quantitative imaging tool to support individualized therapeutic decision-making. The broader clinical applicability of this approach requires further validation through multicenter studies.

**Keywords:** IQon Spectral CT; Prospective Study; Quantitative Parameters; Hepatocellular Carcinoma; Radiotherapy; Treatment Efficacy

## Introduction

HCC is a malignant neoplasm that poses a significant threat to global public health. According to data from the World Health Organization (WHO), approximately 910,000 new cases and 830,000 deaths were attributed to HCC worldwide in 2020 [1]. In China, more than 85% of patients with HCC are not candidates for curative surgical resection due to various factors, including large tumor burden, vascular invasion, underlying chronic hepatitis or cirrhosis, compromised liver function, poor performance status, unfavorable tumor location, or lack of access to liver transplantation. Radiation therapy has become an important local treatment modality based on the principle of radiation-induced cellular damage. With advances in radiotherapy techniques and technology, its therapeutic efficacy has improved substantially, positioning it as a key component in the management of hepatic malignancies [2-4]. The Chinese Guidelines for the Diagnosis and Treatment of Hepatocellular Carcinoma (2024 edition) recommend [3]: For selected patients with stage Ib disease who are ineligible for surgery or ablation, or who decline invasive interventions, external beam radiotherapy may be considered an effective alternative (Evidence Level 2, Recommendation Grade B). Furthermore, combining transarterial chemoembolization (TACE) with external beam radiotherapy can enhance local tumor control

and prolong survival in patients with CNLC stage IIa and IIb HCC. Nevertheless, there remains a lack of imaging-based evaluation strategies specifically designed to assess radiotherapy response in HCC. Currently the assessment of radiotherapy efficacy in HCC primarily relies on conventional response criteria for solid tumors, which evaluate treatment outcomes by measuring the longest diameter of target lesions and assessing changes in contrast enhancement patterns. A major limitation of these criteria is their inability to accurately reflect on the underlying pathological changes following treatment. CT plays a critical role in monitoring HCC; however, conventional CT largely depends on morphological assessments, making it challenging to differentiate viable tumor tissue from post-treatment inflammatory reactions or fibrotic scarring, thereby compromising diagnostic accuracy [5]. Magnetic resonance imaging (MRI) and ultrasound are also commonly used for evaluating treatment response, yet each has inherent limitations. Following radiotherapy, changes in lesion volume may not reliably correlate with therapeutic effect, as radiation-induced necrosis and fibrosis can occur without significant reduction in size. These pathological alterations may not be clearly depicted on MRI, particularly in the presence of hemorrhage or fat deposition, which can lead to complex signal intensities and hinder accurate interpretation. Ultrasound, although widely accessible, is limited by suboptimal spatial resolution and inadequate tissue penetration, potentially failing to detect deep-seated tumors or small residual foci, thus increasing the risk of incomplete assessment of treatment response.

IQon Spectral CT represents a rapidly advancing imaging technology that enables quantitative analysis of tumor internal structure and allows fine characterization of microstructural and hemodynamic changes. This capability facilitates more precise evaluation of tumor response to therapy [6]. In recent years, growing evidence both domestically and internationally has demonstrated the superior diagnostic performance of dual-layer spectral CT in assessing non-surgical treatments across various cancers, including lung cancer [7], gastric cancer [8], and colorectal cancer [9], outperforming conventional CT, MRI, and ultrasound. Therefore, this study aims to investigate the utility of quantitative parameters derived from dual-layer spectral CT in evaluating the efficacy of radiotherapy for HCC. By analyzing multiparametric spectral imaging data collected before and after radiotherapy, and referencing mRECIST, we seek to quantitatively assess pathological responses and establish a reliable imaging-based method for evaluating radiotherapy outcomes in HCC patients.

## Data and Methods

### Study Population

This study enrolled patients diagnosed with hepatocellular carcinoma who received outpatient or inpatient care at the Department of Oncology, Guiping People's Hospital,

between July 2022 and June 2024. After applying predefined inclusion and exclusion criteria, a total of 30 patients were included in the final analysis.

Inclusion criteria: (1) Age  $\geq$  18 years; (2) Confirmed diagnosis of hepatocellular carcinoma based on clinical and imaging standards; (3) Presence of contraindications for surgical resection or patient refusal of surgical intervention; (4) Eligibility for radiotherapy according to multidisciplinary team assessment; (5) Patients without severe comorbidities affecting major organ systems (cardiac, cerebral, pulmonary, or hepatic functional impairment); (6) Expected survival duration  $\geq$  3 months. Exclusion criteria: (1) Patients with secondary (metastatic) liver tumors; (2) Patients with coagulation dysfunction that is difficult to correct clinically; (3) Patients with concurrent systemic diseases or other malignant neoplasms; (4) Patients with contraindications to radiotherapy; (5) Patients lost to follow-up or those with incomplete clinical data. According to the mRECIST evaluation criteria, patients were classified into a response group (CR+PR) and a non-response group (SD+PD). For each patient, imaging data were collected at three time points: before treatment (designated as Group A, control group), after the first treatment cycle (Group B, experimental group 1), and after the second treatment cycle (Group C, experimental group 2), as illustrated in Figure 1.

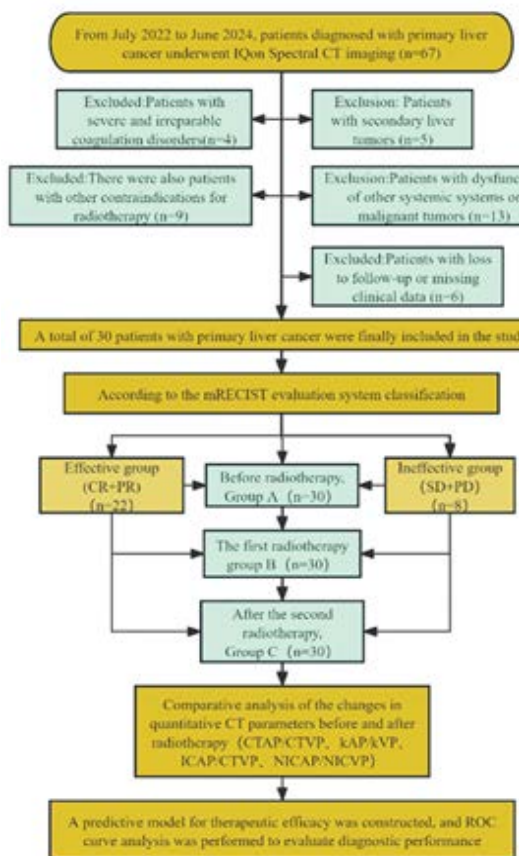


Figure 1

**Citation:** Jin Ying Lan, Jin Han Yang, Dong Wu Chen, Jin Yuan Liao. Predictive Value of Quantitative Parameters in Evaluating Radiotherapy Efficacy for Hepatocellular Carcinoma Based on IQon Spectral CT: A Prospective Study. Journal of Radiology and Clinical Imaging. 9 (2026): 1-9.

## Methods

### Radiotherapy Protocol

A CT scan was performed for tumor localization, during which the gross tumor volume (GTV) was delineated and critical normal tissues within the radiation field were identified. Radiotherapy was delivered using 6 MV-X photons with a prescribed dose of 2 Gy per fraction, administered once daily. The treatment cycle was defined as 21 days, and imaging assessments were conducted over two complete cycles. For patients who completed fewer than two cycles, follow-up imaging was performed up to the last available visit.

### IQon Spectral CT Imaging Protocol

All scans were performed using a Philips IQon Spectral CT system, with both non-contrast and dynamic contrast-enhanced phases, including arterial phase (30s post-injection), portal venous phase (60s), and equilibrium phase (120s). Scanning parameters were as follows: collimation of  $0.625 \times 64$  mm, reconstruction of conventional and single-energy images with slice thickness and interval of 5 mm, and thin-slice conventional and spectral data images reconstructed at 1 mm thickness and spacing. Reconstruction algorithm: iDose<sup>4</sup>; gantry rotation speed: 0.5 s/rotation; pitch: 1.0; tube voltage: 120kV; tube current: 340–520 mA. The contrast agent used was iodixanol injection (300 mgI/mL; Yangtze River Pharmaceutical Group Co, Ltd.). Total iodine dose was individualized based on body surface area, with injection flow rate calculated as total volume divided by 20 seconds. This was followed by a 10-second saline flush at the same flow rate. The scanning range extended from approximately 20 mm above the diaphragm to the level of the iliac crest. Bolus tracking was initiated at a region of interest placed ~20 mm above the diaphragm, with a trigger threshold set at 100 Hounsfield units (HU). Subsequent acquisitions were timed as follows: late arterial phase at 12s post-trigger, portal venous phase at 32s, equilibrium phase at 52s, and delayed phase at 285s. All scans were performed during breath-hold after full inspiration, with patients trained in consistent breath-holding techniques prior to examination.

### Image Analysis Parameters

**Qualitative assessment:** Enhancement patterns within the lesion were evaluated using effective atomic number pseudocolor maps from arterial and portal phases (color scale: red  $\rightarrow$  orange  $\rightarrow$  green  $\rightarrow$  blue, representing high to low enhancement) to assess residual viable tumor tissue. Additionally, spectral curve slope analysis (transition from steep to flat slopes indicating progression from viable tissue to necrosis) during arterial or portal phases was used to determine tumor viability in regions with heterogeneous enhancement.

**Quantitative assessment:** Lesion size measurements were obtained for each patient at three time points—before

radiotherapy, after the first cycle, and after the second cycle. CT attenuation values (in HU) of the lesion and adjacent normal liver parenchyma were recorded during enhanced arterial and portal phases across all three examinations. Iodine concentration (IC) of the lesion, normal liver parenchyma, and abdominal aorta was measured on iodine density maps during the arterial and portal phases. The NIC was calculated for each phase as  $NIC = IC_{lesion} / IC_{aorta}$ . Changes in the effective atomic number of the lesion were also analyzed across the three time points to reflect compositional changes.

### Evaluation of Therapeutic Response

Therapeutic efficacy was assessed via IQon Spectral CT imaging before radiotherapy (Group A), after the first cycle (Group B), and after the second cycle (Group C), based on predefined spectral CT response criteria. Tumor control was evaluated by integrating morphological, enhancement, and quantitative spectral parameters.

### Observation Indicators

#### Imaging Parameters

1. Maximum diameter (mm) of the target lesion was measured on both unenhanced and contrast-enhanced images across three time points.
2. CT attenuation values (HU) of the lesion and normal liver parenchyma were recorded during each contrast phase.
3. The diameter (in millimeters) and iodine uptake of both the lesion and normal liver parenchyma were measured on contrast-enhanced iodine density maps at each imaging phase, and the NIC of the lesion was calculated for each phase using the formula:  $NIC = IC_{lesion} / IC_{aorta}$ . Lesion diameter (mm) and relative effective atomic number values were recorded on effective atomic number maps at three distinct time points. Additionally, the slope of the spectral curve during the arterial and portal venous phases of contrast-enhanced scanning was analyzed—specifically, the k-value of the spectral curve—with a transition from steep to flat indicating tissue necrosis, whereas sustained steepness suggested residual viable tumor.

#### Efficacy Evaluation Criteria

**CR:** At the conclusion of two treatment cycles, all target lesions exhibited no enhancement in the arterial phase or pseudocolor enhancement on effective atomic number maps. Iodine uptake on iodine density maps did not exceed that of normal liver parenchyma, and the spectral curve slope changed from steep to flat, consistent with complete tumor necrosis.

**PR:** A reduction of at least 30% in the sum of diameters of target lesions during the arterial phase of contrast-enhanced imaging; a decrease of no less than 30% in both lesion diameter and relative effective atomic number on effective

atomic number maps; and a corresponding  $\geq 30\%$  reduction in lesion diameter and iodine uptake on iodine density maps, accompanied by a change in the spectral curve slope from steep to gentle, indicative of partial tumor necrosis.

**SD:** Changes in target lesions that do not meet the criteria for either PR or PD, with no significant alteration in size or enhancement characteristics.

**PD:** An increase of at least 20% in the diameter of target lesions during the arterial phase compared to baseline; an increase of at least 20% in lesion diameter on effective atomic number maps without a significant change in relative atomic number; a  $\geq 20\%$  increase in lesion diameter with unchanged iodine uptake on iodine density maps; the appearance of new intrahepatic lesions or distant lymph node metastases; and a reversal of the spectral curve slope from flat or gentle to steep, suggesting tumor regrowth.

The objective response rate (ORR) was calculated as (number of patients with CR+PR) divided by the total number of patients, multiplied by 100%. Patients were classified into either the response group (CR+PR) or the non-response group (SD+PD).

Statistical analyses were conducted using SPSS 25.0 software. For normally distributed continuous variables with homogeneity of variance, data are presented as mean  $\pm$  standard deviation ( $\bar{X} \pm SD$ ), and intergroup comparisons across three time points were performed using one-way repeated measures analysis of variance (ANOVA). Categorical variables are expressed as percentages (%), and between-group comparisons were carried out using the chi-square test. The significance level was set at  $\alpha = 0.05$  for all tests, with two-tailed probability values applied. A  $p$ -value  $< 0.05$  was considered statistically significant. ROC curves were constructed to assess the diagnostic performance of quantitative spectral CT parameters in predicting treatment response and to develop a predictive model for therapeutic efficacy.

### Results

#### Overall Treatment Response in 30 HCC Patients

A total of 30 patients with hepatocellular carcinoma (clinical stages II–IV) were enrolled in the study. Based on post-radiotherapy response assessment, patients were classified into a response group (CR+PR) and a non-response group (SD+PD). Among these patients, 3 achieved CR, 19 achieved PR, 5 exhibited SD, and 3 developed PD.

#### Changes in Spectral CT Parameters Before and After Treatment

Prior to radiotherapy, the NICAP was significantly higher in the response group than in the non-response group ( $P < 0.05$ ). No significant differences were observed in other baseline parameters between the two groups ( $P > 0.05$ ). Following the first and second cycles of radiotherapy, the

response group demonstrated significant reductions in CT attenuation (CTAP/CTVP), spectral slope (kAP/kVP), ICAP/ICVP and NICAP/NICVP compared to baseline values (all  $P<0.05$ ). In contrast, these parameters did not show statistically significant decreases in the non-response group ( $P>0.05$ ), and some even increased. Significant intergroup differences were observed after treatment for parameters including CTAP, kAP, and ICAP ( $P<0.05$ ), as summarized in Tables 1 and 2.

Note: CTAP/VP denotes the CT attenuation value (in HU) of lesions in the arterial or portal venous phase; kAP/VP refers to the spectral curve slope in the respective phase; ICAP/VP represents iodine concentration (mg/mL) during the arterial or portal venous phase; NICAP/VP indicates normalized iodine concentration. Asterisks indicate statistically significant differences between the response and non-response groups.

**This study constructed five prediction models to evaluate the therapeutic efficacy of radiotherapy for hepatocellular carcinoma**

The AUC of the KAP\_ICAP model was 0.642 (95% CI: 0.410-0.874). The AUC of the KAP\_NICAP model was 0.886 (95% CI: 0.759-1), that of the ICAP\_NICAP model was 0.898 (95% CI: 0.778-1), and that of the KAP\_ICAP\_NICAP model was 0.915 (95% CI: 0.814-1), with a sensitivity of 86.4% and a specificity of 87.5%. The DeLong test showed that the predictive performance of this model was significantly better than that of the KAP\_ICAP model ( $Z = -2.3960$ ,  $P = 0.017$ ), but there was no statistically significant difference compared with other bivariate models ( $P>0.05$ ). This study used the ensemble learning method (stacking) to construct a combined prediction model, with an AUC of 0.915 (95% CI: 0.810-1), a sensitivity of 90.9%, a specificity of 87.5%, a positive predictive value of 95.2%, and a negative predictive value of 77.8%. The DeLong test indicated that the combined prediction model had no significant difference in predictive performance from the three-variable model ( $P = 0.999$ ) but was significantly better than the KAP\_ICAP model ( $Z = -2.3621$ ,  $P = 0.018$ ). As summarized in Tables 3, Figures 2 and Figures 3 (A1-E1, A2-E2, and A3-E3).

**Table 1:** Changes in IQon Spectral CT Parameters of Patients in the Effective Group Before and After Radiotherapy.

Parameters	Effective Group (CR+PR) (n=22)				
	Before Radiotherapy, Group A	The first Radiotherapy, Group B	After the second Radiotherapy, Group C	t	P
CTAP (HU)	112.45±27.10	89.62±21.07*	86.23±18.77*	4.009	<0.001
CTVP (HU)	90.45±18.20	81.05±15.44	81.23±17.05	2.542	0.017
kAP	1.76±0.35	1.25±0.28*	1.23±0.24*	2.71	0.006
kVP	1.96±0.52	1.61±0.43	1.57±0.41	2.488	0.019
ICAP (mg/ml)	1.31±0.35	0.97±0.16*	0.98±0.20*	3.125	0.004
ICVP (mg/ml)	1.50±0.42	1.29±0.38	1.27±0.25	2.124	0.04
NICAP	0.18±0.07*	0.08±0.04	0.08±0.03	1.342	0.197
NICVP	0.35±0.14	0.19±0.06	0.18±0.07	2.351	0.023

Note: CTAP/VP denotes the CT attenuation value (in HU) of lesions in the arterial or portal venous phase; kAP/VP refers to the spectral curve slope in the respective phase; ICAP/VP represents iodine concentration (mg/mL) during the arterial or portal venous phase; NICAP/VP indicates normalized iodine concentration. Asterisks indicate statistically significant differences between the response and non-response groups.

**Table 2:** Changes in IQon Spectral CT Parameters of Patients in the Ineffective Group Before and After Radiotherapy.

Parameters	Ineffective Group (SD+PD) (n=8)				
	Before Radiotherapy, Group A	The first Radiotherapy, Group B	After the second Radiotherapy, Group C	t	P
CTAP (HU)	117.81±33.24	107.62±26.54	104.33±21.07	1.875	0.092
CTVP (HU)	92.30±23.06	85.17±18.26	83.89±15.21	1.214	0.23
KAP	1.58±0.47	1.43±0.38	1.44±0.29	1.221	0.218
KVP	1.88±0.50	1.75±0.43	1.70±0.37	1.57	0.142
ICAP (mg/ml)	1.20±0.41	1.22±0.35	1.16±0.31	0.245	0.673
ICVP (mg/ml)	1.45±0.42	1.34±0.29	1.32±0.24	0.792	0.368
NICAP	0.09±0.04	0.08±0.04	0.07±0.02	0.31	0.582
NICVP	0.27±0.10	0.22±0.08	0.21±0.12	0.825	0.33

**Table 3:** Five predictive models for evaluating the therapeutic effect of radiotherapy on HCC.

Model	AUC	Sensitivity	Specificity	95%CI	PPV	NPV
kAP-ICAP	0.642	0.364	1	0.41-0.874	1	0.364
kAP-NICAP	0.886	0.909	0.75	0.759-1	0.909	0.75
ICAP-NICAP	0.898	0.864	1	0.778-1	1	0.727
kAP-ICAP-NICAP	0.915	0.864	0.875	0.814-1	0.95	0.7
Combined	0.915	0.909	0.875	0.81-1	0.952	0.778

**Note:** The AUC of the KAP\_ICAP model was 0.642 (95% CI: 0.410-0.874). The AUC of the KAP\_NICAP model was 0.886 (95% CI: 0.759-1), that of the ICAP\_NICAP model was 0.898 (95% CI: 0.778-1), and that of the KAP\_ICAP\_NICAP model was 0.915 (95% CI: 0.814-1).

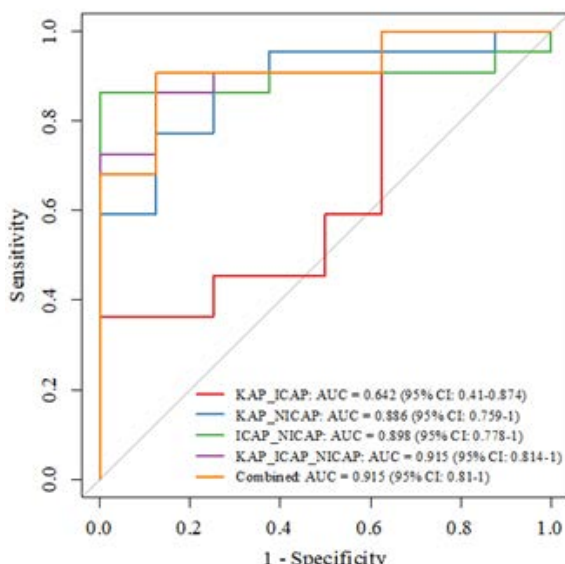


**Figure 2:** ROC curve analysis of kAP, ICAP, and NICAP in the effective group before radiotherapy.

**Note:** In conclusion, the model incorporating NICAP parameters demonstrates high accuracy in predicting the therapeutic efficacy of radiotherapy for hepatocellular carcinoma. The three-variable combined model and the ensemble learning combined prediction model both exhibit excellent predictive performance and can provide reliable quantitative tools for clinical assessment of radiotherapy efficacy.

## Discussion

IQon Spectral CT offers notable advantages in evaluating the therapeutic efficacy of radiotherapy for HCC. By discriminating between mixed-energy X-ray photons, IQon Spectral CT enables simultaneous acquisition of multi-energy images with a slice thickness of 1 mm, thereby enhancing lesion contour delineation and improving visualization of anatomical structures. This modality provides a comprehensive set of quantitative parameters—including CT attenuation values, spectral slope (k-values), IC, NIC, and effective atomic number—which serve as objective biomarkers for assessing treatment response. Analysis of ICAP and ICVP reflects changes in tumor iodine uptake, indirectly indicating alterations in tumor vascularity and metabolic activity. NIC, which is normalized

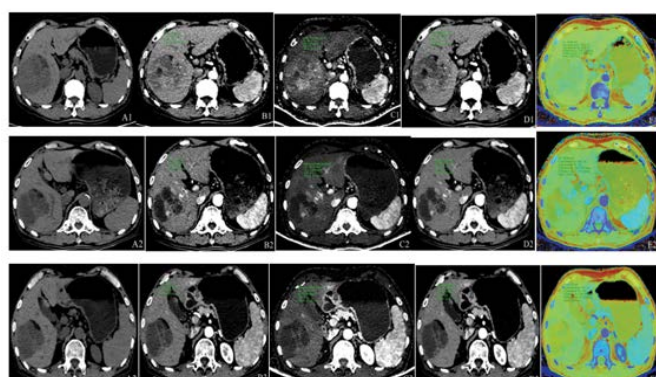


**Figure 3:** Male patient, 67 years old, with giant hepatocellular carcinoma. Panels A1–A3 represent unenhanced CT images; B1–B3, conventional arterial-phase images; C1–C3, iodine density maps in the arterial phase; D1–D3, spectral images at 40 keV in the arterial phase; and E1–E3, effective atomic number maps in the arterial phase. Panels A1–E1 display pre-radiotherapy imaging findings: unenhanced CT reveals a large, heterogeneous hypodense mass in the right hepatic lobe; arterial-phase imaging shows marked enhancement; iodine density mapping demonstrates a region of high iodine uptake; low-energy spectral imaging (40 keV) clearly delineates the lesion with well-defined margins; and atomic number mapping reveals predominantly light green signal intensity within the tumor. Panels A2–E2 depict imaging findings after the first cycle of radiotherapy: compared to baseline, there is a reduction in lesion size, density, enhancement extent, iodine uptake area, and solid components, with concomitant expansion of cystic necrotic regions. Panels A3–E3 illustrate post-second-cycle radiotherapy imaging: further reduction in tumor size and enhancement range is observed, iodine uptake is nearly absent, solid components are minimal, and the necrotic component has expanded.

to the iodine concentration in the abdominal aorta, reduces inter-individual variability and allows for more accurate assessment of tissue perfusion. These quantitative metrics support personalized treatment planning by integrating tumor-specific characteristics, hepatic functional status, and radiation tolerance to optimize radiation dosing and scheduling. Longitudinal monitoring using IQon Spectral CT facilitates real-time evaluation of therapeutic efficacy and prognosis prediction through comparative analysis of pre- and post-treatment imaging data. In our study, pre-radiotherapy NICAP values demonstrated significant discriminatory ability between responders and non-responders (AUC=0.88,

95% CI: 0.76–1,  $P<0.05$ ), highlighting their clinical utility in HCC management. Furthermore, pathological response assessment is essential for refining radiotherapy strategies in HCC. By monitoring tumor shrinkage, necrosis, and fibrosis, clinicians can dynamically adjust treatment protocols to enhance therapeutic outcomes. IQon Spectral CT provides quantitative parameters for the precise assessment of treatment responses in HCC. CT attenuation values reflect changes in tissue density, serving as direct indicators of tumor response to radiotherapy. The energy slope (k-value) of the spectral curve correlates with tumor differentiation status; studies have demonstrated that well-differentiated HCC exhibits significantly lower k-values compared to poorly differentiated tumors, enabling non-invasive grading and informing treatment planning [14,15]. Although the k-value alone does not determine radiotherapy efficacy, it contributes valuable insights into tumor biology. IC serves as a marker of tumor vascularization and potential radiosensitivity, as higher IC—associated with richer tumor vascularity—indicates increased angiogenesis and enhanced radiation sensitivity due to iodine's radiosensitizing properties. NIC, which adjusts IC relative to a reference standard, minimizes inter-individual variability and facilitates cross-patient comparisons for evaluating angiogenesis and radiosensitivity [13].

In clinical practice, the integration of parameters such as k-value, IC, and NIC supports the development of personalized treatment strategies. For example, patients exhibiting low k-values and high IC may be candidates for intensified radiotherapy regimens. Serial imaging during treatment offers real-time monitoring of tumor dynamics; significant changes—such as decreasing CT values or reduced NICAP—may indicate tumor regression or emerging resistance, thereby guiding timely adjustments to therapeutic protocols [14,15]. In this study, the effective treatment group demonstrated tumor shrinkage and decreased CT values following radiotherapy, consistent with tumor regression or necrosis. Notably, NIC, particularly NICAP, exhibited strong predictive performance for treatment response (AUC = 0.88, 95% CI: 0.76–1,  $P<0.05$ ), aligning with findings from previous studies [13]. Tumor size remains an independent prognostic factor for clinical outcomes [15]. Collectively, IQon Spectral CT derived parameters not only reflect underlying tumor pathology but also support treatment optimization and efficacy evaluation by integrating quantitative imaging biomarkers with tumor characteristics and clinical data.

This study presents a systematic investigation of multi-parameter features derived from IQon Spectral CT in assessing radiotherapy efficacy for HCC, proposing a non-invasive predictive model based on these quantitative indices. In contrast to prior reports, this work specifically compares CT attenuation values obtained at different energy levels (40 keV vs. 70 keV), revealing that images reconstructed at 40 keV yield significantly higher CT values and superior predictive

accuracy for therapeutic response [16]. IQon Spectral CT parameters—including energy-dependent CT attenuation and NIC offer distinct advantages in capturing tissue energy heterogeneity and pathological characteristics. These metrics enable precise quantification of lesion properties such as vascularization and cellular density, which are essential for accurate treatment evaluation. Moreover, IQon Spectral CT's capacity to differentiate and quantify heterogeneous tissue components enhances the detection and characterization of HCC-related pathological changes, including necrosis and fibrosis [17]. The combination of multi-energy imaging and quantitative analysis establishes a robust framework for non-invasive, real-time monitoring of treatment outcomes in HCC. Furthermore, IQon Spectral CT demonstrates significant utility in HCC evaluation by enabling virtual monoenergetic reconstruction from spectral data, allowing for reduced radiation dose without compromising diagnostic image quality [18]. In addition to conventional CT imaging, IQon Spectral CT generates spectral parameter maps—including virtual monochromatic images and material-specific density maps—that enhance the characterization of HCC biological behavior and treatment response. Spectral analysis improves diagnostic accuracy by resolving subtle differences between HCC lesions and surrounding normal liver parenchyma. Ultrasound, a non-invasive and radiation-free imaging modality, is widely utilized for the early detection of HCC due to its cost-effectiveness and capacity for real-time visualization of hepatic anatomy and hemodynamics. It also facilitates image-guided interventions such as radiofrequency ablation and microwave coagulation therapy, thereby enhancing procedural accuracy and safety. However, diagnostic performance is highly dependent on operator expertise and equipment quality, with small tumors ( $<1\text{cm}$ ), particularly those located in anatomically challenging regions—such as near the diaphragm or in subcostal areas—frequently overlooked. MRI complements these approaches by providing high-resolution characterization of HCC microstructure, including the detection of small lesions and assessment of vascular invasion. Multi-sequence MRI with contrast enhancement enables comprehensive evaluation of tumor function and metabolism. Diffusion-weight imaging (DWI) plays a particularly important role in monitoring radiotherapy response. DWI measures the diffusion of water molecules within tissues, reflecting dynamic changes in tumor cellularity: prior to radiotherapy, high cellular density results in reduced apparent diffusion coefficient (ADC) values; following treatment, necrosis and edema lead to increased ADC values; and tumor recurrence is typically associated with a subsequent decline in ADC. This capability allows for real-time, non-invasive assessment of therapeutic efficacy.

DWI demonstrates high diagnostic accuracy in the characterization of hepatocellular carcinoma, especially for small lesions, where its sensitivity and specificity exceed those of conventional MRI sequences. This advantage stems

from DWI's ability to detect cytological alterations through restricted water diffusion, enabling reliable differentiation between benign and malignant hepatic lesions. During radiotherapy, DWI enhances diagnostic precision by capturing temporal changes in tumor biology: recurrent disease commonly presents with decreased ADC values, whereas radiation-induced necrosis is characterized by stable or elevated ADC levels. This distinction is clinically significant, as marked increases in ADC suggest favorable treatment response and support continuation of the current regimen, while minimal or declining ADC values may indicate resistance and warrant dose modification or consideration of alternative therapies. Although MRI offers superior diagnostic performance in HCC evaluation through high spatial resolution and multiparametric analysis, its widespread use is limited by high costs and contraindications in patients with metallic implants. In contrast, IQon Spectral CT generates spectral parameter maps—including material decomposition images and quantified iodine concentration—that enable assessment of HCC biological behavior and treatment response at a lower cost. Ultrasound remains valuable for frequent monitoring due to its real-time capabilities and economic feasibility, yet it is constrained by operator dependence and limited sensitivity for small or deeply situated lesions. These modalities are complementary: IQon Spectral CT emphasizes quantitative material characterization, MRI provides functional and molecular insights, and ultrasound excels in real-time procedural guidance. Evidence supports the utility of IQon Spectral CT in evaluating non-surgical cancer treatments. Baxa et al. [16] reported significant reductions in arterial- and venous-phase IC among responders with non-small cell lung cancer, with the most pronounced decrease observed in the venous phase. Meng Dejie et al. [17] validated IQon Spectral CT in advanced gastric cancer, identifying significant differences in venous-phase IC, IC change rates, and CT attenuation values between treatment responders and progressors. Wu Meihong et al. [18] further confirmed the predictive value of IQon Spectral CT for chemotherapy response in lung cancer, demonstrating that pre-treatment NICAP correlates with short-term therapeutic outcomes. These findings are consistent with the results of the present study, reinforcing the potential of IQon Spectral CT as a non-invasive, multi-parametric tool for monitoring oncologic treatment response.

In summary, IQon Spectral CT parameters—including CT attenuation values, energy slope  $k$ , IC, and NIC—provide effective means of assessing lesion status and tumor radiosensitivity [14,15]. Notably, NICAP exhibits strong predictive performance for radiotherapy efficacy, a finding that aligns with previous reports in non-small cell lung cancer and gastric cancer [16,17]. Nevertheless, this study has several limitations, including a relatively small sample size and limited population heterogeneity [18], which may affect the generalizability of the results. Future research should aim

to validate the diagnostic and prognostic utility of NICAP in larger, multicenter, and more diverse patient cohorts to establish its robustness in guiding HCC management.

## Author Contributions

All authors contributed to the study conception and design. Material preparation, data collection and analysis were performed by Jin Ying Lan, Jin Han Yang, Dong Wu Chen and Jin Yuan Liao. The first draft of the manuscript was written by Jin Ying Lan, Jin Han Yang and Dong Wu Chen, and all authors commented on previous versions of the manuscript. All authors have read and approved the final version of the manuscript.

## Acknowledgement

I would like to affirm all the glory, honor and praise be to the Majesty God, who endowed me health, insight and strength in the whole write up process.

The authors would like to thank the Department of Radiology at Guiping People's Hospital.

My appreciation also goes out to Dr. Jin Yuan Liao, my colleague and my family, particularly Jin Han Yang and Dong Wu Chen, who provided me unreserved encouragement and support.

## Recommendations

We recommend multicenter prospective studies that include a more diverse patient cohort, such as individuals with varying liver function grades and tumor stages, to further refine the parameters, validate their generalizability, and ultimately facilitate their integration into clinical practice as a decision-support tool for guiding individualized radiotherapy in hepatocellular carcinoma.

## Disclosure

The authors of this manuscript have no conflict of interest and there is no financial disclosure to be made.

## Institutional Review Board and confidentiality Statement

Authors of this manuscript declare that they have followed the ethical standards of the institution on the publication process.

## Funding

This work was supported by the Guangxi Zhuang Autonomous Region Health Commission (Grant No. Z-R 20221961) and the Guiding Research Fund of Guiping People's Hospital.

## Informed Consent Statement

Informed consent was obtained from all participants.

**Data Availability Statement:** Excluded.**References**

1. Ferlay J, Colombet M, Soerjomataram I, et al. Cancer statistics for the year 2020: An overview. *Int J Cancer* (2021).
2. Bray F, Laversanne M, Sung H, et al. Global cancer statistics 2022: GLOBOCAN estimates of incidence and mortality worldwide for 36 cancers in 185 countries. *CA Cancer J Clin* 74 (2024): 229-263.
3. Zhou J, Sun H, Wang Z, et al. Guidelines for the Diagnosis and Treatment of Primary Liver Cancer (2022 Edition). *Liver Cancer* 12 (2023): 405-444.
4. Sanuki N, Takeda A, Tsurugai Y, et al. Role of stereotactic body radiotherapy in multidisciplinary management of liver metastases in patients with colorectal cancer. *Jpn J Radiol* 40 (2022): 1009-1016.
5. Taylor N, Renfrew H. Does Dose Matter? Ionizing Radiation Exposure of the Veterinary Patient From Computed Tomography: A Discussion. *Top Companion Anim Med* 51 (2022): 100697.
6. Greffier J, Villani N, Defez D, et al. Spectral CT imaging: Technical principles of dual-energy CT and multi-energy photon-counting CT. *Diagn Interv Imaging* 104 (2023): 167-177.
7. Wen LJ, Zhao QY, Yin YH, et al. Application value of double-layer spectral detector CT in differentiating central lung cancer from atelectasis. *Ann Palliat Med* 11 (2022): 1990-1996.
8. Hong Y, Zhong L, Lv X, et al. Application of spectral CT in diagnosis, classification and prognostic monitoring of gastrointestinal cancers: progress, limitations and prospects. *Front Mol Biosci* 10 (2023): 1284549.
9. Yuan X, Quan X, Che XL, et al. Preoperative prediction of the lymphovascular tumor thrombus of colorectal cancer with the iodine concentrations from dual-energy spectral CT. *BMC Med Imaging* 23 (2023): 103.
10. De la Pinta C. Toward Personalized Medicine in Radiotherapy of Hepatocellular Carcinoma: Emerging Radiomic Biomarker Candidates of Response and Toxicity. *OMICS* 25 (2021): 537-544.
11. Öcal O, Schinner R, Schütte K, et al. Early tumor shrinkage and response assessment according to mRECIST predict overall survival in hepatocellular carcinoma patients under sorafenib. *Cancer Imaging* 22 (2022): 1.
12. Ilaria, Vicentin, Cristina et al. Inter-center agreement of mRECIST in transplanted patients for hepatocellular carcinoma. [J] *European radiology*, 2021, 31(2021): 8903-8912.
13. Bhandari A, Koppen J, Wastney T, et al. A systematic review and meta-analysis of spectral CT to differentiate focal liver lesions. *Clin Radiol* 78 (2023): 430-436.
14. Sauerbeck J, Adam G, Meyer M. Spectral CT in Oncology. *Onkologische Bildgebung mittels Spektral-CT*. *Rofo* 195 (2023): 21-29.
15. Kruis MF. Improving radiation physics, tumor visualisation, and treatment quantification in radiotherapy with spectral or dual-energy CT. *J Appl Clin Med Phys* 23 (2022): e13468.
16. Baxa J, Matouskova T, Krakorova G, et al. Dual-Phase Dual-Energy CT in Patients Treated with Erlotinib for Advanced Non-Small Cell Lung Cancer: Possible Benefits of Iodine Quantification in Response Assessment. *Eur Radiol* 26 (2016): 2828-2836.
17. Meng Dejie, Liu Yang, Wang Libing, et al. The value of spectral double-layer detector CT iodine content quantitative prediction and evaluation of the treatment effect of advanced gastric cancer [J]. *Journal of Medical Imaging* 31 (2021): 1200-1219
18. Wu Meihong, Li Xiaohu, Sheng Mao, et al. The evaluation value of dual layer detector spectral CT for the short-term efficacy of chemotherapy in patients with advanced lung cancer [J]. *Chinese Journal of Clinical Medical Imaging* 33 (2022): 700-703



This article is an open access article distributed under the terms and conditions of the Creative Commons Attribution (CC-BY) license 4.0